

## The stability of the $O^{(N)}$ invariant fixed point in three dimensions

This article has been downloaded from IOPscience. Please scroll down to see the full text article.

1998 J. Phys. A: Math. Gen. 31 4603

(<http://iopscience.iop.org/0305-4470/31/20/004>)

View [the table of contents for this issue](#), or go to the [journal homepage](#) for more

Download details:

IP Address: 171.66.16.122

The article was downloaded on 02/06/2010 at 06:52

Please note that [terms and conditions apply](#).

## The stability of the $O(N)$ invariant fixed point in three dimensions

M Caselle<sup>†§</sup> and M Hasenbusch<sup>‡||</sup>

<sup>†</sup> Dipartimento di Fisica Teorica dell'Università di Torino, Istituto Nazionale di Fisica Nucleare, Sezione di Torino, via P Giuria 1, I-10125 Torino, Italy

<sup>‡</sup> Humboldt Universität zu Berlin, Institut für Physik, Invalidenstr. 110, D-10099 Berlin, Germany

Received 25 November 1997

**Abstract.** We study the stability of the  $O(N)$  fixed point in three dimensions under perturbations of the cubic type. We address this problem in the three cases  $N = 2, 3, 4$  by using finite-size scaling techniques and high-precision Monte Carlo simulations. It is well known that there is a critical value  $2 < N_c < 4$  below which the  $O(N)$  fixed point is stable and above which the cubic fixed point becomes the stable one. Whilst we cannot exclude that  $N_c < 3$ , as recently claimed, our analysis strongly suggests that  $N_c$  coincides with 3.

### 1. Introduction

Quantum field theories with  $\phi^4$  type interactions are of importance in several physical contexts. In particular, they represent one of the most powerful tools in the study of critical phenomena [1]. Due to their simplicity they allow perturbative expansions up to rather large orders from which one can extract estimates for various critical quantities (critical indices and amplitude ratios) comparable in precision with those of the most advanced Monte Carlo simulations. In the simplest case the theory contains a single field  $\phi$  and describes the Ising universality class (for a recent comparison between field theoretic and Monte Carlo predictions see for example [2]).

When the field  $\phi$  has more than one component the situation becomes more complex and different quartic interaction terms can be defined. The simplest one has the form  $(\sum_{i=1}^N \phi_i^2)^2$ . It is  $O(N)$  symmetric and describes the  $O(N)$  universality class to which belongs, for instance, the isotropic  $N$ -component Heisenberg ferromagnet. Besides this term, the most interesting additional contribution is  $\sum_{i=1}^N \phi_i^4$  which breaks the  $O(N)$  symmetry but preserves the cubic invariance. The cubic subgroup of  $O(N)$  is composed of permutations and reflections of the  $N$  components of the field. Note that in the following ‘cubic’ always refers to the symmetry and not to a third power. The importance of the cubic term is due to the fact that in a real crystal the crystalline structure gives rise to anisotropies which are mainly of the cubic type. Thus real crystals are better described by mixed actions in which both the  $O(N)$  and the cubic term are present.

Besides this phenomenological reason, this mixed model is also interesting in that it is a simple non-trivial QFT with different fixed points in competition among them. In fact, it is

<sup>§</sup> E-mail address: caselle@to.infn.it

<sup>||</sup> E-mail address: hasenbus@birke.physik.hu-berlin.de

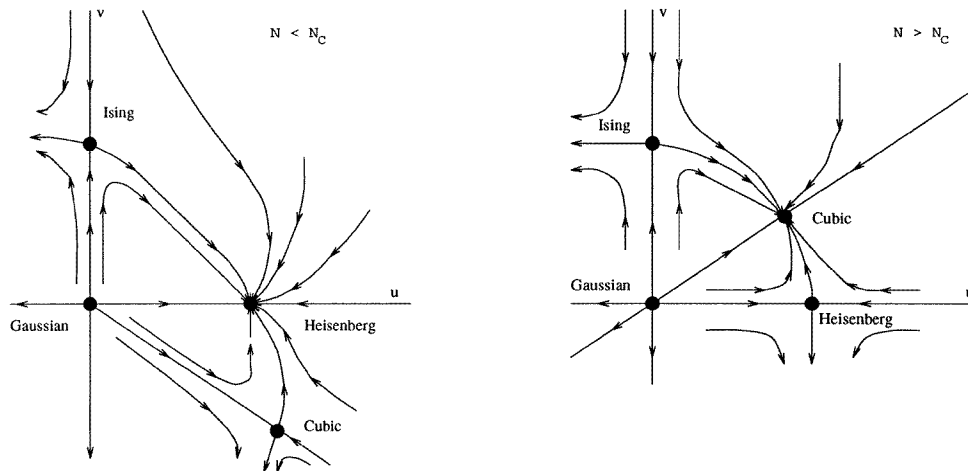


Figure 1. Renormalization group flows for the cubic model in three dimensions.

easy to see that in this model there are four possible fixed points: the trivial Gaussian one, the Ising one (which corresponds to the situation in which the  $N$  components  $\phi_i$  decouple), the  $O(N)$  symmetric and the cubic one (see figure 1). It was shown in [3] that while the Gaussian and Ising fixed points are always unstable, the  $O(N)$  and cubic points interchange their role as  $N$  increases. For  $N < N_c$  the  $O(N)$  symmetric point is stable, while for  $N > N_c$  it is destabilized by the cubic interaction and the cubic fixed point becomes the stable one (see figure 1). It is possible to see within the framework of the  $\epsilon$ -expansion that in three dimensions  $N_c < 4$ . The common lore, (supported by  $\epsilon$ -expansion up to the third order) has always been that  $N_c$  should lie somewhere between 3 and 4 in three dimensions, thus implying that the  $N = 3$  case, which is the most interesting one for applications to real crystals, should have a stable  $O(3)$  symmetric fixed point.

Recently, this commonly accepted scenario has been contrasted in a series of papers [4–8] which suggested that  $N_c$  should lie *below* 3. As a consequence the critical behaviour of magnetic transitions in real crystals should be described by the cubic symmetric fixed point, a result which, if confirmed, would be of relevant interest from a theoretical point of view.

The aim of this paper is to test this conjecture with a high-precision Monte Carlo simulation. By studying finite-size corrections of a cubic invariant perturbation term exactly at the critical  $O(N)$  point we can extract the eigenvalues of the stability matrix of the  $O(N)$  fixed point. We study the three interesting cases  $N = 2, 3, 4$ . For  $N = 2$  and  $N = 4$  the expected results (stability of the isotropic and cubic fixed point respectively) are immediately visible from the data. In the  $N = 3$  case our results imply that  $N_c \approx 3$ . Obviously the numerical simulation cannot determine whether  $N_c = 3$  is an exact result. However, we obtain an upper bound for the absolute value of the stability index  $|b_2|$  for the  $O(3)$  fixed point, which turns out to be impressively small. In particular we are able to exclude all the existing estimates [4, 5, 9–12] except that of Kleinert *et al* [6–8], which is still compatible with our result within one standard deviation.

## 2. The cubic model

We are interested in the three-dimensional quantum field theory defined by the Lagrangian

$$\mathcal{L} = \frac{1}{2} \sum_{i=1}^N (\partial_\mu \phi_i \partial^\mu \phi_i + m^2 \phi_i^2) + \frac{\lambda}{4!} \left( \sum_{i=1}^N \phi_i^2 \right)^2 + \frac{\mu}{4!} \sum_{i=1}^N \phi_i^4. \quad (1)$$

While the term  $(\sum_{i=1}^N \phi_i^2)^2$  is  $O(N)$  symmetric, the term  $\sum_{i=1}^N \phi_i^4$  is only invariant under the ‘cubic’ subgroup composed by permutations and reflections of the  $N$  components  $\phi_i$ . This model is discussed in detail in several quantum field theory textbooks, for example [1].

In the following we shall review the first-order results in the  $\epsilon$ -expansion. This rather simple approximation already gives all the qualitative features of the renormalization flows of the model.

The fixed points of the theory are given by the zeros of the  $\beta$ -functions. The stability matrices are given by the derivatives of the  $\beta$ -functions at the zeros. From the eigenvalues of these matrices it is then easy to identify the stable fixed point.

The two  $\beta$ -functions are given, at the first-order in the  $\epsilon$ -expansion, by

$$\beta_u = -\epsilon u + u^2 \frac{N+8}{6} + uv \quad (2)$$

$$\beta_v = -\epsilon v + \frac{3}{2} v^2 + 2uv \quad (3)$$

where  $u$  and  $v$  are the renormalized couplings related to  $\lambda$  and  $\mu$  respectively.

By looking at the zeros of the  $\beta$ -functions one can see that there are four possible fixed points:

- (1) The Gaussian fixed point  $u = 0 \quad v = 0$ .
- (2) The Ising fixed point  $u = 0 \quad v = \frac{2}{3}\epsilon$ .
- (3) The Heisenberg ( $O(N)$  invariant) fixed point  $u = \frac{6}{N+8}\epsilon \quad v = 0$ .
- (4) The cubic fixed point  $u = \frac{2}{N}\epsilon \quad v = \frac{2(N-4)}{3N}\epsilon$ .

The stability matrix is defined as

$$B = \begin{pmatrix} \frac{\partial \beta_u(u,v)}{\partial u} & \frac{\partial \beta_u(u,v)}{\partial v} \\ \frac{\partial \beta_v(u,v)}{\partial u} & \frac{\partial \beta_v(u,v)}{\partial v} \end{pmatrix}. \quad (4)$$

At the first order of the  $\epsilon$ -expansion one obtains

$$B = \begin{pmatrix} -\epsilon + \frac{N+8}{3}u + v & u \\ 2v & -\epsilon + 2u + 3v \end{pmatrix}. \quad (5)$$

The corresponding eigenvalues, evaluated at the four fixed points are as follows.

- (1) Gaussian:  $b_1 = b_2 = -\epsilon$ .
- (2) Ising:  $b_1 = -\frac{\epsilon}{3} \quad b_2 = \epsilon$ .
- (3) Heisenberg:  $b_1 = \epsilon \quad b_2 = \frac{4-N}{N+8}\epsilon$ .
- (4) cubic fixed point:  $b_1 = N\epsilon \quad b_2 = \frac{N-4}{3}\epsilon$ .

It is easy to see that the Gaussian and Ising fixed points are always unstable, independently from the value of  $N$ . In particular the Ising fixed point has only one direction of instability, while the Gaussian one is unstable in both directions.

The cubic and  $O(N)$  fixed points interchange their role as a function of  $N$ . For  $N$  smaller than a critical value  $N_c$  (which at this order in the  $\epsilon$ -expansion turns out to be 4) the Heisenberg fixed point is the stable one and defines the universality class towards which the system flows in the infrared limit.

For  $N > N_c$ ,  $b_2$  evaluated at the Heisenberg point becomes negative while  $b_2$  evaluated at the cubic fixed point becomes positive and the cubic fixed point becomes the stable one.

The renormalization flows corresponding to these two situations are reported in figure 1. For  $N < N_c$  all initial points with  $u > 0$  and  $v > \frac{N-4}{3}u$  will flow towards the  $O(N)$ -invariant, Heisenberg fixed point. For  $N > N_c$  all initial points with  $u > 0$  and  $v > 0$  will flow in the infrared limit towards the cubic fixed point which, for  $N < N_c$  lies in the  $v < 0$  half-plane, exactly at  $N = N_c$  crosses the  $v = 0$  axis and moves for  $N > N_c$  in the  $v > 0$  region.

Initial points outside the above defined regions flow away towards more negative values of  $u$  and/or  $v$  and finally reach the region in which the positivity condition for the quartic potential is no longer satisfied. These trajectories are related (from the statistical mechanics point of view) to realizations of the cubic model in which the phase transition is of the fluctuation-induced first-order type. These models have recently attracted much interest as a laboratory to study arbitrary weak first-order transitions [14].

The last remaining point is to find the value of  $N_c$  in three dimensions. It is easy to see by looking to higher orders in the  $\epsilon$ -expansion, or with the help of Monte Carlo simulations, that for  $N = 2$  the Heisenberg fixed point is stable and that in contrast for  $N = 4$  the cubic fixed point is the stable one. Thus  $2 < N_c < 4$ . However, it is difficult to decide whether  $N_c$  is greater or lower than 3. Equivalently one can look at the sign of the  $b_2$  eigenvalue at the Heisenberg point for  $N = 3$ . If  $b_2$  is positive, then  $N_c$  must be greater than 3. During the last 20 years many efforts have been made to settle this question. The first result was reported in [9] where the  $\epsilon$ -expansion for  $N_c$  was extended up to the third-order leading to the estimate  $N_c = 3.128$ . In agreement with this estimate (but, using a completely different approach), Grover *et al* [10] obtained  $b_2 = 0.053$  at  $N = 3$ . A few years later, using different approximation techniques, the two contrasting results:  $N_c \sim 2.3$  [11] and  $N_c \sim 3.4$  [12] were obtained. Ten years later in [4, 5] a value  $N_c < 3$  was suggested. In particular in [5], by means of a three loop calculation directly in  $d = 3$ , the values  $N_c = 2.91$  and  $b_2 = -0.008$  were proposed. Finally, more recently, Kleinert *et al* pushed the  $\epsilon$ -expansion up to the fifth order [7] and obtained a similar answer. First, in [7] they found, (with a [2,2] Padé approximant)  $N_c = 2.958$ . Then in [8], by using a careful resummation procedure of the fifth-order series, they obtained the value  $b_2 = -0.00214$  for the stability eigenvalue at  $N = 3$ . In [13], using the same series of [7], but a different resummation procedure, the value  $N_c = 2.855$  was found. Due to the nature of these results it is very difficult to add sensible error bars to these estimates. However, it is clear from the above discussion that the existing estimates for  $N_c$  are scattered around  $N_c = 3$  and that as the various techniques and approximations become increasingly more refined the corresponding estimates for  $N_c$  becoming closer to  $N_c = 3$ .

### 3. The simulation

#### 3.1. The model

The cubic model discussed in section 2 has a simple and straightforward lattice realization, defined by the action:

$$S = -\beta \sum_{\langle xy \rangle} s_x s_y - \mu \sum_x \sum_{i=1}^N (s_x^i)^4 \quad (6)$$

where  $s_x$  is a unit vector in  $R^N$ .  $\langle x, y \rangle$  denotes a pair of nearest-neighbour sites on the lattice. We consider a three-dimensional cubic lattice of size  $L$  and lattice spacing  $a = 1$ . For  $\mu = 0$  we have the standard  $O(N)$  invariant (Heisenberg) model, while for  $\mu \neq 0$  the cubic-invariant perturbation  $\sum_x \sum_{i=1}^N (s_x^i)^4$  breaks the  $O(N)$  symmetry. In the following

**Table 1.** Results for  $\beta_c$  given in the literature for  $N = 2$ .

Ref.	Method	$\beta_c$
[15]	MCRG	0.454 20(2)
[15]	MC	0.454 170(7)
[16]	MC	0.454 165(4)
[17]	HT	0.454 19(3)

**Table 2.** Results for  $\beta_c$  given in the literature for  $N = 3$ .

Ref.	Method	$\beta_c$
[18]	MC	0.693 0(1)
[19]	MC	0.693 1(1)
[20]	MC	0.693 035(37)
[16]	MC	0.693 002(12)
[17]	HT	0.693 03(3)
[17]	HT- $\theta$	0.693 05(4)

**Table 3.** Results for  $\beta_c$  given in the literature for  $N = 4$ .

Ref.	Method	$\beta_c$
[21]	MC	0.936 0(1)
[16]	MC	0.935 861(8)
[17]	HT	0.935 89(6)
[17]	HT- $\theta$	0.935 93(6)

we shall study this model in the three cases  $N = 2, 3, 4$ . We shall concentrate our main efforts on the  $N = 3$  case.

In three dimensions, for  $\mu = 0$ , the  $O(N)$  model undergoes a second-order phase transition for some value  $\beta_c$  (which depends on  $N$ ) of the coupling. In the vicinity of such a point the continuum limit can be taken, leading to the  $O(N)$  symmetric QFT (corresponding to the  $v = 0$  axis in figure 1) discussed in the previous section. The presence of such a continuous phase transition is obviously a mandatory condition for the whole analysis.

The simplest way to extract the value of  $N_c$  from a lattice simulation is to determine the stability eigenvalues  $b_2$  for  $N = 3$ . From the lattice point of view the  $b_2$  eigenvalue appears as the critical index which controls the behaviour of any cubic-invariant (but  $O(N)$ -violating) observable in the vicinity of the Heisenberg transition point.

The most efficient way to evaluate such a critical index is to look at the finite-size dependence (as a function of the lattice size  $L$ ) of a suitable observable (to be defined below) evaluated exactly at the critical point  $\beta_c$ . Thus it is necessary to have a good estimate of the critical coupling. Fortunately,  $\beta_c$  is known with high precision in each of the three cases  $N = 2, 3, 4$  in which we are interested. This is one of the reasons why we have chosen this particular lattice realization of the cubic model.

In tables 1–3 we have collected the most recent results for  $\beta_c$  both from Monte Carlo simulations and from series expansions. HT- $\theta$  indicates the biased resummation of the HT series in which the value of the index  $\theta$  is given as input parameter. It is interesting to see that all the estimates agree within the errors.

**Table 4.** Values of  $\beta_c$  used in this paper.

$N$	$\beta_c$
2	0.454 165(4)
3	0.693 002(12)
4	0.935 861(8)

In table 4 we report the values (chosen from table 1–3) that we used in our simulations.

### 3.2. Observables

There are four natural observables in the model (6). The two terms which appear in the action:

$$E \equiv \sum_{\langle xy \rangle} s_x s_y \quad (7)$$

and

$$P \equiv \sum_x \sum_i (s_x^i)^4. \quad (8)$$

The total magnetization, which is the order parameter of the transition:

$$M \equiv \sum_x s_x \quad (9)$$

and the ratio

$$R = \frac{\sum_i (M^i)^4}{(M^2)^2} \quad (10)$$

which quantifies the violation of the  $O(N)$  symmetry in the model<sup>†</sup>.

In order to study the stability of the fixed point we are actually interested in the derivative of  $\langle R \rangle$  with respect to  $\mu$  at  $\beta = \beta_c$  and  $\mu = 0$ :

$$D_R \equiv \left. \frac{\partial \langle R \rangle}{\partial \mu} \right|_{\mu=0, \beta=\beta_c}. \quad (12)$$

In fact this derivative measures the (generalized) susceptibility of the system with respect to a cubic perturbation, such as what happens for the ordinary magnetic susceptibility in the case of a magnetic perturbation or for the specific heat in the case of a thermal perturbation. At this point, a standard finite-size scaling analysis tells us that the critical index which measures the infrared stability of the system with respect to the above perturbations, also controls the finite-size behaviour (namely the  $L$ -dependence) of the corresponding susceptibility exactly at the critical point. In particular, in the case in which we are interested,  $D_R$  should behave for  $\beta = \beta_c$  and  $\mu = 0$ , as

$$D_R \propto L^{-b_2} \quad (13)$$

<sup>†</sup> Other choices are possible for the latter observable. For instance the term

$$X = \frac{M_{\max}^2}{M^2} \quad (11)$$

where  $M_{\max}^2$  is the maximal square of a component of the magnetization would work equally well. However, it turns out that the ratio  $R$  defined above is the one which can be measured in the most efficient and simple way.

where  $b_2$  is exactly the stability eigenvalue of the Heisenberg fixed point that we are looking for.

Scaling laws of the type (13) are expected to hold for sufficiently large values of  $L$ . For small lattices, correction to scaling terms should be expected. It is thus important to have results with small statistical errors for large lattice sizes. A few preliminary tests have demonstrated that (at least for the case  $N = 3$ ) sizes up to  $L = 32$  are needed to extract reliable estimates of  $b_2$ . This requirement represents the major technical problem of this work.

There are two possible choices to compute  $D_R$ .

- It can be computed directly in the simulation at  $\mu = 0$  as

$$D_R = \langle PR \rangle - \langle P \rangle \langle R \rangle. \quad (14)$$

- It can be computed by using the finite-difference method, i.e. by simulating the model at small non-zero values of  $\mu$ :

$$D_R(\mu) \equiv \frac{R(\mu) - R(-\mu)}{2\mu}. \quad (15)$$

It is easy to recover the relationship between  $D_R$  and  $D_R(\mu)$ . First, let us notice that on a finite lattice  $R(\mu, \beta)$  must be an analytic function of its parameters. This holds also at  $\beta = \beta_c$ . Therefore we can Taylor-expand  $R(\mu, \beta)$  in powers of  $\mu$  for fixed  $\beta = \beta_c$ . Taking the symmetric difference we obtain

$$D_R = D_R(\mu) + \frac{1}{3!} \frac{d^3 R}{d\mu^3} \mu^2 + O(\mu^4). \quad (16)$$

Both definitions have their drawbacks. The  $\mu = 0$  simulations are affected by a strong enhancement of the variance (hence of the statistical errors) as  $L$  increases. It ensues that the statistical error of  $D_R$  at a fixed number of measurements increases roughly as  $L^{3/2}$ . As a consequence excessively large samples are needed to keep the error sufficiently small for  $L > 16$ .

In contrast, for  $D_R(\mu)$  at fixed  $\mu$  the statistical error does not increase with  $L$ . However, the  $O(\mu^2)$  corrections do increase with  $L$ . Reducing these  $O(\mu^2)$  corrections requires a reduction in the value of  $\mu$ . This in turn requires an increase in the number of measurements to keep the statistical error fixed.

In the following section we shall discuss a way of avoiding these problems. By using the global  $O(N)$  symmetry of the model at  $\mu = 0$  an improved version of  $D_R$  can be constructed. This improvement does not change the  $L$  dependence of the variance, but gives a significant reduction of its magnitude, thus allowing us to reach, with a reasonable CPU time, lattice sizes as large as  $L = 32$  which are large enough to extract the finite-size behaviour with the required precision. Most of the data that we shall discuss in the final section were obtained by using this improved observable. We also performed, as a cross check, some simulations at finite  $\mu$ . The agreement that we find between the values of  $D_R$  obtained in these two ways is a non-trivial check of the reliability of our results.

### 3.3. Variance-reduced estimator for $D_R$ .

Variance-reduced estimators have the same expectation value as the corresponding standard estimators. However, their variance is reduced, which allows for more accurate results in Monte Carlo simulations than the standard estimator. A general principle to construct variance reduced estimators is to look for degrees of freedom which can be integrated out analytically.



In order to obtain a variance reduced estimator of  $\frac{\partial \langle R \rangle}{\partial \mu}$  we integrate  $P, R$  and  $PR$  over the global  $O(N)$  rotations.

This is trivial for  $P$  and  $R$ , but it is less simple in the case of the  $PR$  component. Since  $P$  is a sum over all lattice sites we can commute the integration over the global rotations and the summation over the lattice sites. The integral to be solved is hence given by

$$I = \int_{O(N)} DT \left( \sum_i [(Ts_x)^i]^4 \right) \left( \sum_i [(Tm)^i]^4 \right) \quad (17)$$

where  $T$  is an element of  $O(N)$ ,  $DT$  the Haar-measure,  $s_x$  the spin at the site  $x$ , and  $m$  a unit vector in the direction of the global magnetization. For symmetry reasons the integral only depends on the angle between  $s_x$  and  $m$ , which we define as follows

$$ms_x = \cos(\alpha). \quad (18)$$

Integral (17) can be evaluated explicitly for any value of  $N$ . Details of the calculation are reported in the appendix. Here we only list the results in the three cases in which we are interested:

$$N = 2$$

$$I = \frac{9}{16} + \frac{1}{32} \cos(4\alpha) \quad (19)$$

$$N = 3$$

$$I = \frac{1}{60} \cos(4\alpha) + \frac{1}{105} \cos(2\alpha) + \frac{153}{420} \quad (20)$$

$$N = 4$$

$$I = \frac{2}{25} \cos^4(\alpha) - \frac{3}{50} \cos^2(\alpha) + \frac{51}{200}. \quad (21)$$

### 3.4. The Monte Carlo algorithm

Due to the different symmetries in the models, we had to use different algorithms in the two cases  $\mu = 0$  and  $\mu \neq 0$ .

**3.4.1.  $\mu = 0$**  In the case  $\mu = 0$  we used the single-cluster algorithm of Wolff [22] and the microcanonical overrelaxation algorithm. The basic idea of the cluster algorithm is to construct conditional Ising models. This is achieved by allowing only the sign-change of the spin component parallel to a unit vector  $r$  in  $R^N$ . The delete probability depends on the pair of lattice sites and is given by

$$p_d(x, y) = \min[1, \exp(-2(rs_x)(rs_y))] \quad (22)$$

where  $x$  and  $y$  are nearest-neighbour sites on the lattice. The vector  $r$  is chosen with a probability density uniform on  $S^{N-1}$ . For each update a new  $r$  is chosen.

The variance of the improved estimator of  $D_R$  is mainly caused by local fluctuations of the spins. Hence it is useful to supplement the cluster-algorithm with a fast local algorithm to produce local changes of the configuration. For that purpose we used the microcanonical overrelaxation algorithm.

The elementary update of the algorithm is given by

$$s'_x = \frac{2(n_x s_x) n_x}{n_x^2} - s_x \quad (23)$$

where  $n_x$  is the sum of the nearest-neighbour spins of  $s_x$ . Since neither a random number nor the evaluation of the exponential function is needed for this update the CPU-time required is rather small compared with a Metropolis or a heat-bath update.

The whole update cycle used in our simulations consists of a mixture of nine overrelaxation sweeps and  $K$  cluster updates.  $K$  is chosen such that the number of spins updated in  $K$  cluster updates is of the order of the number of lattice sites. A measurement is performed after each overrelaxation sweep and after the cluster-updates. There are hence 10 measurements in the nine overrelaxation sweeps and  $K$  cluster-updates cycle.

3.4.2.  $\mu \neq 0$ . For  $\mu \neq 0$  some modifications are needed. We have restricted the vector  $r$  such that  $\sum_i (s^i)^4$  is not altered by the update. This is guaranteed if the sign of a component is changed or two components are exchanged or a combination of both. This means that  $r$  is either parallel to an axis or is diagonal in a plane.

$r$  is in

$$(1, 0, \dots, 0), (0, 1, \dots, 0) \cdots (0, 0, \dots, 1) \quad (24)$$

or

$$\frac{1}{\sqrt{2}}(1, 1, \dots, 0), \frac{1}{\sqrt{2}}(1, 0, \dots, 1), \dots \frac{1}{\sqrt{2}}(0, \dots, 1, 1) \quad (25)$$

or

$$\frac{1}{\sqrt{2}}(1, -1, \dots, 0), \frac{1}{\sqrt{2}}(1, 0, \dots, -1), \dots \frac{1}{\sqrt{2}}(0, \dots, 1, -1). \quad (26)$$

While this restriction of  $r$  to a discrete subset of  $S^{N-1}$  does not violate detailed balance it means that the cluster update by itself is not ergodic.

In order to restore ergodicity we supplement the cluster update with an (ergodic) Metropolis update. For performance reasons we also added a local reflection update that is microcanonical for  $\mu = 0$ . A spin is reflected at the sum of its neighbours

$$s'_x = \frac{(S_x s_x) S_x}{S_x^2} - 2s_x \quad (27)$$

where  $S_x$  is the sum of the spins on nearest-neighbour sites of  $x$ . For  $\mu \neq 0$  the proposal  $s'_x$  is accepted with a probability

$$P_{\text{acc}} = \min \left[ 1, \exp \left( \mu \sum_i [(s'_x)^4 - (s_x^i)^4] \right) \right]. \quad (28)$$

A whole update cycle consists of one Metropolis update, one local reflection update plus  $K$  cluster updates.  $K$  is chosen, as in the  $\mu = 0$ , case such that the number of spins updated in  $K$  cluster updates is of the order of the number of lattice sites. A measure is performed in each update cycle.

### 3.5. Statistical and systematic errors

We evaluated statistical errors with the standard binning method. Both in the  $\mu = 0$  and  $\mu \neq 0$  cases bins of 1000 update cycles are chosen (corresponding to 10 000 and 1000 measurements respectively). This binning was already performed during the simulation since not all individual measurements could be stored on disc. Besides the statistical uncertainty we also have to face the systematic error due to the uncertainty  $\Delta\beta_c$  in the estimate of  $\beta_c$ . To evaluate this error we also measured in the simulation the expectation value  $\langle ER \rangle$ . The difference

$$\langle ER \rangle - \langle E \rangle \langle R \rangle \quad (29)$$

gives an estimate of the derivative of  $\langle R \rangle$  with respect to  $\beta$ , from which we can obtain the systematic error induced on  $R$  by the uncertainty in  $\beta_c$ :

$$(\langle ER \rangle - \langle E \rangle \langle R \rangle) \times \Delta\beta_c. \quad (30)$$

With a similar construction we obtain the error induced on  $D_R$ . We can consider this as a lower bound on the accuracy that we can reach for the derivatives. It makes no sense to reduce the statistical error of  $D_R$  below this bound. This observation fixes the typical sample size for the simulations, which was of the order of 20 000 bins.

## 4. Results and discussion

### 4.1. Results at $\mu = 0$

We simulated the models with  $N = 2, 3, 4$  at  $\mu = 0, \beta = \beta_c$ , in the ranges  $L \in [4 - 16]$  for  $N = 2$ ;  $L \in [4 - 32]$  for  $N = 3$  and  $L \in [4 - 20]$  for  $N = 4$ . The results are reported in tables 5–7. In the first column we report the lattice size and in the second the values of the derivative  $D_R$ . The first error in parenthesis denotes the statistical uncertainty, while in the second parenthesis the error induced by the uncertainty in  $\beta_c$  is reported. In the last column we report the sample size (number of bins multiplied by the number of measurements in each bin).

### 4.2. Results at $\mu \neq 0$

As a test of the above results we also performed simulations at  $\mu \neq 0$ , both for  $N = 2$  and  $N = 3$ . We evaluated the finite  $\mu$  estimators  $D_R(\mu)$  by using equation (15). The

**Table 5.** Results for  $D_R$  in the  $N = 2$  model.

$L$	$D_R$	Statistics
4	0.011 046(20)(1)	$10\,000 \times 10^4$
6	0.010 506(34)(2)	$10\,000 \times 10^4$
8	0.010 121(51)(2)	$10\,000 \times 10^4$
10	0.009 728(58)(4)	$15\,000 \times 10^4$
12	0.009 523(76)(5)	$15\,000 \times 10^4$
16	0.008 904(117)(4)	$15\,000 \times 10^4$

**Table 6.** Results for  $D_R$  in the  $N = 3$  model.

$L$	$D_R$	Statistics
4	0.019 672(19)(3)	$10\,000 \times 10^4$
6	0.020 118(19)(5)	$15\,000 \times 10^4$
8	0.020 187(20)(7)	$20\,004 \times 10^4$
10	0.020 196(25)(10)	$20\,870 \times 10^4$
12	0.020 152(32)(13)	$21\,500 \times 10^4$
14	0.020 178(40)(15)	$20\,770 \times 10^4$
16	0.020 233(49)(16)	$20\,750 \times 10^4$
20	0.020 094(68)(22)	$20\,150 \times 10^4$
24	0.020 178(84)(28)	$23\,145 \times 10^4$
32	0.020 265(140)(39)	$19\,560 \times 10^4$

**Table 7.** Results for  $D_R$  in the  $N = 4$  model.

$L$	$D_R$	Statistics
4	0.023 474(15)(1)	$10\,000 \times 10^4$
6	0.025 287(16)(3)	$10\,000 \times 10^4$
8	0.026 294(19)(4)	$10\,000 \times 10^4$
10	0.027 097(23)(6)	$10\,000 \times 10^4$
12	0.027 742(27)(8)	$10\,600 \times 10^4$
16	0.028 774(39)(13)	$10\,000 \times 10^4$
20	0.029 605(52)(38)	$10\,050 \times 10^4$

**Table 8.** Results for  $D_R$  for  $\mu \neq 0$ .

	$N = 2, L = 8$	$N = 2, L = 12$	$N = 2, L = 16$	$N = 3, L = 12$
$\mu = 4$		0.010 503(140)(3)		
$\mu = 2$	0.010 117(28)(1)	0.010 008(122)(3)		
$\mu = 1$	0.010 112(57)(1)	0.009 495(118)(3)		0.020 977(64)(9)
$\mu = 0.5$	0.010 054(74)(1)	0.009 505(103)(3)	0.009 139(103)(4)	0.020 306(130)(9)
$\mu = 0.25$				0.020 076(257)(9)
$\mu = 0$	0.010 121(51)(2)	0.009 523(76)(5)	0.008 904(117)(4)	0.020 152(32)(13)

results are reported in table 8 where, in the last line, we also reported for comparison the corresponding  $\mu = 0$  estimates.

The agreement between the results obtained from the two approaches is very good and makes us confident about the reliability of the  $\mu = 0$  set of data.

#### 4.3. The $b_2$ index

We fitted the data obtained at  $\mu = 0$  with the scaling law

$$D_R = CL^{-b_2}. \quad (31)$$

The fit results are collected in table 9 where in the second column we give the minimum value  $L_{\min}$  of  $L$  taken into account in the fit. In the third and fourth columns we report the reduced  $\chi^2$  and the confidence level respectively. Finally, the last two columns report the best fit values of  $C$  and  $b_2$ . As usual we give in the first parenthesis the statistical error and in the second the error induced by  $\beta_c$ . The various fits are plotted and compared in figure 2 and 3.

The large value of  $\chi^2$  clearly indicates that for any value of  $N$  the sample at  $L = 4$  is strongly affected by correction to scaling terms and must be discarded. Fits without  $L = 4$  have an acceptable  $\chi^2$ . However, this fact does not necessarily imply that it is justified to ignore corrections to scaling. Hence we regard the fits with  $L_{\min} = 8$  as our final result. Still it remains difficult to quantify the systematic error due to corrections to scaling. Based on the experience with the finite-size scaling analysis of other exponents of the Heisenberg model we expect them to be of the same order of magnitude as the statistical error of the  $L_{\min} = 8$  fits.

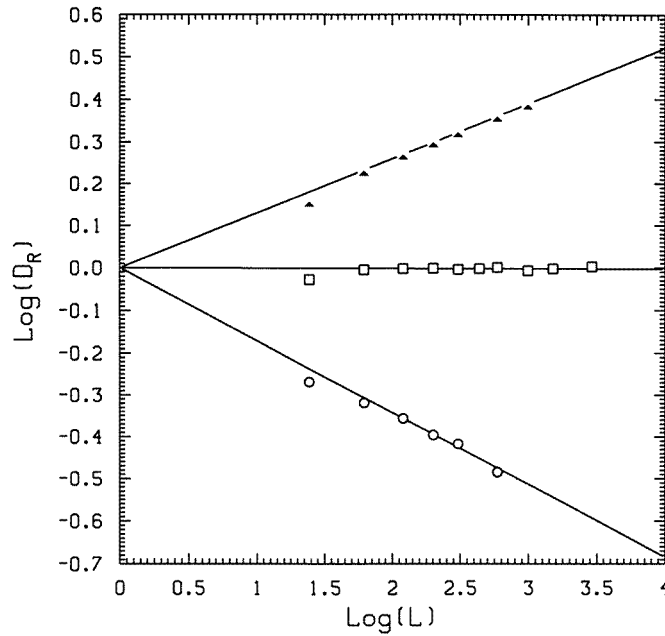


**Figure 2.**  $\text{Log}(D_R)$  as a function of  $\text{Log}(L)$ . Triangles, squares and circles denote the  $N = 4$ ,  $N = 3$  and  $N = 2$  data respectively. Errors are not reported since they are smaller than the symbol sizes. To render easier the comparison among the three sets of data, all the values of  $D_R$  have been normalized to the best fit value of the constant  $C$  (see table 9 for the value of  $C$ ). The three lines correspond to the best fits obtained neglecting the  $L = 6$  derivative.

**Table 9.** Results for  $C$  and  $b_2$ .

$N$	$L_{min}$	$\chi^2_{red}$	CL (%)	$C$	$b_2$
2	4	2.01	9	0.013 35(9)(1)	0.1362(40)(3)
2	6	1.17	32	0.013 81(24)(1)	0.1519(84)(4)
2	8	0.85	43	0.014 45(54)(2)	0.1711(166)(6)
3	4	26.5	0	0.019 36(4)(2)	-0.0174(10)(6)
3	6	1.32	23	0.020 05(6)(2)	-0.0026(14)(7)
3	8	0.71	64	0.020 22(10)(3)	0.0007(20)(9)
4	4	77.5	0	0.019 28(3)(1)	-0.1473(7)(4)
4	6	1.22	30	0.019 97(5)(2)	-0.1321(10)(5)
4	8	0.51	67	0.020 08(8)(3)	-0.1299(16)(8)

#### 4.4. Discussion and comparison with other estimates

As can be seen from table 9, our results for  $N = 3$  are certainly incompatible with all the existing estimates [4, 5, 9–12], except that of Kleinert *et al* [6–8]. In fact, if we keep in the fit for  $N = 3$  also the  $L = 6$  sample we find an impressive agreement with the result  $b_2 = -0.002 14$  of [7]. However, as mentioned above, we strongly suspect that the  $L = 6$  sample is still affected by correction to scaling terms and prefer to quote as our best estimate the  $L = [8-32]$  result  $b_2 = 0.0007(20)(9)$ , which is still compatible with the result of [7], but suggests that  $N_c$  could indeed exactly coincide with 3. In this respect it must also be

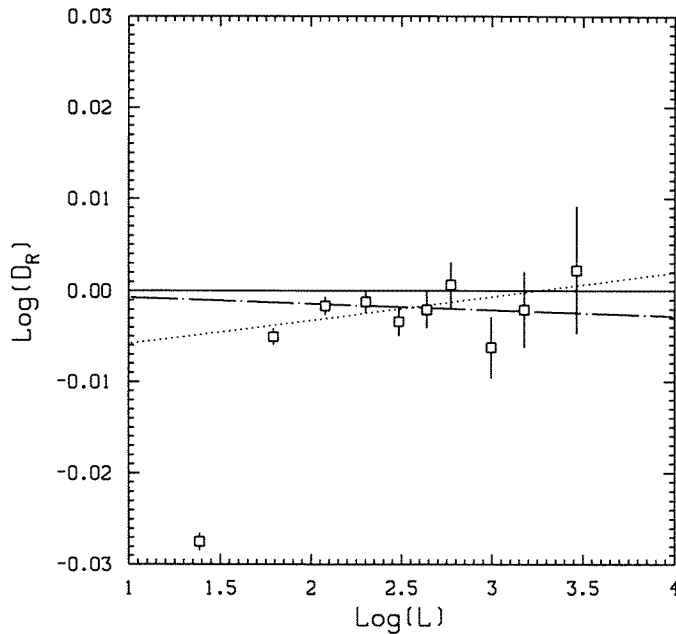


**Figure 3.** The  $N = 3$  data only, plotted with a much higher resolution. The dotted line corresponds to the best fit including  $L = 6$ , while the broken line corresponds to the  $L = [8-32]$  fit. All the points are normalized as in figure 2.

noticed that the trend of the perturbative estimates of  $b_2$  quoted in [7] as a function of the order in the perturbative expansion also suggests that  $N_c$  converges to 3 in agreement with our result.

In any case, let us stress again that it is obviously impossible to determine by means of a numerical simulation whether  $N_c = 3$  is an exact result and that the fact that the difference  $|N_c - 3|$  is so small, and compatible with zero, might well be a coincidence. However, we think that it would be worthwhile to look for an argument which explains why the cubic and Heisenberg fixed point in three dimensions should coincide exactly for  $N = 3$ .

### Acknowledgments

We thank F Gliozzi, G Münster, K Pinn, P Provero and S Vinti for many helpful discussions. Work supported in part by the European Commission TMR programme ERBFMRX-CT96-0045.

### Appendix

In this appendix we evaluate the integral

$$I = \int_{O(N)} DT \left( \sum_i [(T s_x)^i]^4 \right) \left( \sum_i [(T m)^i]^4 \right) \quad (\text{A1})$$

where  $T$  is an element of  $O(N)$ ,  $DT$  the Haar-measure,  $s_x$  the spin at the site  $x$  and  $m$  a unit vector in the direction of the global magnetization. For symmetry reasons the integral

only depends on the angle between  $s_x$  and  $m$  which is defined as

$$ms_x = \cos(\alpha). \quad (\text{A2})$$

We write the integral as

$$I(\alpha) = \int_{S^{N-1}} ds \left( \sum_i s_i^4 \right) \int_{S^{N-2,s}} dt \left( \sum_i t_i^4 \right) \quad (\text{A3})$$

where  $\int_{S^{N-1}}$  denotes the integral over the  $N$ -dimensional sphere.  $\int_{S^{N-2,s}}$  denotes the integral over the  $N - 1$  dimensional subspace defined as the set of all the vectors  $t$  that for any fixed  $s$  satisfy the equation  $st = \cos(\alpha)$ . We choose the normalizations so that  $\int_{S^{N-1}} ds = 1$  and  $\int_{S^{N-2,s}} dt = 1$ .

Because of symmetry we can restrict the calculation to the first component of  $s$

$$I(\alpha) = N \int_{S^{N-1}} ds s_1^4 \int_{S^{N-2,s}} dt \left( \sum_i t_i^4 \right). \quad (\text{A4})$$

Now we decompose the integral  $\int_{S^{N-1}}$  into the integral over the  $s_1$  component and for fixed  $s_1$  over the remaining  $S^{N-2}$ .

We obtain

$$I(\alpha) = N \text{ constant} \int_{s_1=0}^{s_1=1} ds_1 (1 - s_1^2)^{(N-3)/2} s_1^4 \int_{S^{N-2}} ds' \int_{S^{N-2,s}} dt \left( \sum_i t_i^4 \right) \quad (\text{A5})$$

where

$$\text{constant}_1 = \left[ \int_{s_1=0}^{s_1=1} ds_1 (1 - s_1^2)^{(N-3)/2} \right]^{-1} \quad (\text{A6})$$

and  $s'$  is  $s$  without the 1-component.

Let us now study

$$\int_{S^{N-2}} ds' \int_{S^{N-2,s}} dt. \quad (\text{A7})$$

This measure for  $t$  is invariant under rotations around the 1-axis. The non-trivial question is the measure for the 1-component of  $t$ . The range of  $t_1$  is given by

$$t_{\max} = \cos(\alpha)s_1 + \sin(\alpha)\sqrt{1 - s_1^2} \quad (\text{A8})$$

and

$$t_{\min} = \cos(\alpha)s_1 - \sin(\alpha)\sqrt{1 - s_1^2}. \quad (\text{A9})$$

The measure between these extreme values is given by the fact that for any  $s$ ,  $t$  is distributed on a  $S^{N-2}$  sphere. Hence the measure is (for  $N > 2$ )

$$\text{constant}_2 \left[ 1 - \left( \frac{t_1 - c}{2s} \right)^2 \right]^{(N-4)/2} \quad (\text{A10})$$

with  $c = \cos(\alpha)s_1$  and  $s = \sin(\alpha)\sqrt{1 - s_1^2}$ . The normalization constant<sub>2</sub> is given by

$$\text{const}_2 = \left\{ \int_{t_1=c-s}^{c+s} \left[ 1 - \left( \frac{t_1 - c}{2s} \right)^2 \right]^{(N-4)/2} dt_1 \right\}^{-1}. \quad (\text{A11})$$

For fixed  $t_1$  the integration of the remaining components gives us

$$(1 - t_1^2)^2 \langle R \rangle_{N-1}, \text{ with } \langle R \rangle_N = 3/(N + 2).$$

Now we are in the position to write down the full integral:

$$I(\alpha) = N \text{ constant}_1 \int_{s_1=0}^{s_1=1} ds_1 (1 - s_1^2)^{(N-3)/2} s_1^4 \quad (\text{A12})$$

$$\text{constant}_2 \int_{t_1=c-s}^{c+s} \left[ 1 - \left( \frac{t_1 - c}{2s} \right)^2 \right]^{(N-4)/2} \left( t_1^4 + \frac{3}{N+1} (1 - t_1^2)^2 \right). \quad (\text{A13})$$

This integral can be solved with standard techniques and yields in the three cases  $N = 2, 3, 4$ . The results are listed in section 3.

## References

- [1] See for instance Amit D J 1989 *Field Theory, the Renormalization Group and Critical Phenomena* 2nd edn (Singapore: World Scientific)
- Zinn-Justin J 1996 *Quantum Field Theory and Critical Phenomena* 3rd edn (Oxford: Clarendon)
- [2] Caselle M and Hasenbusch M 1997 *J. Phys. A: Math. Gen.* **30** 4963
- [3] Aharony A 1973 *Phys. Rev. B* **8** 4270
- [4] Mayer I O and Sokolov A I 1987 *Izv. Akad. Nauk SSSR Ser. Fiz.* **51** 2103  
Mayer I O, Sokolov A I and Shalaye B N 1989 *Ferroelectrics* **95** 93
- [5] Shpot N A 1989 *Phys. Lett. A* **142** 474
- [6] Kleinert H and Thoms S 1995 *Phys. Rev. D* **52** 5926
- [7] Kleinert H and Schulte-Frohlinde V 1995 *Phys. Lett. B* **342** 284
- [8] Kleinert H, Thoms S and Schulte-Frohlinde V *Preprint quant-ph/9611050*
- [9] Ketley I J and Wallace D J 1973 *J. Phys. A: Math. Gen.* **6** 1667  
Nelson D R, Kosterlitz J M and Fisher M E 1974 *Phys. Rev. Lett.* **33** 813
- [10] Grover M K, Kadanoff L P and Wegner F J 1972 *Phys. Rev. B* **6** 311
- [11] Yalabik M C and Houghton A 1977 *Phys. Lett.* **61A** 1
- [12] Newman K E and Riedel E K 1982 *Phys. Rev. B* **25** 264
- [13] Shalaev B N, Antonenko S A and Sokolov A I 1997 *Phys. Lett. A* **230** 105
- [14] See for instance Tetradis N *Preprint hep-th/9706088* and references therein
- [15] Gottlob A and Hasenbusch M 1993 *Physica* **201A** 593
- [16] Ballestreros H G, Fernandez L A, Martin-Mayor V and Munoz Sodupe A 1996 *Phys. Lett. B* **387** 125
- [17] Butera P and Comi M 1997 *Phys. Rev. B* **56** 8212
- [18] Holm C and Janke W 1993 *Phys. Rev. B* **48** 936
- [19] Brown R G and Ciftan M 1996 *Phys. Rev. Lett.* **76** 1352
- [20] Chen K, Ferrenberg A M and Landau D P 1993 *Phys. Rev. B* **48** 3249
- [21] Kanaya K and Kaya S 1995 *Phys. Rev. D* **51** 2404
- [22] Wolff U 1989 *Phys. Rev. Lett.* **62** 361